

PROCEEDINGS OF THE SYMPOSIUM ON

SENSOR SCIENCE AND TECHNOLOGY

April 6-8, 1987
Electronics Design Center
Case Western Reserve University
Cleveland, Ohio 44106

Proceedings Editors
B. Schumm, Jr., C. C. Liu, R. A. Powers, and E. B. Yeager

Sponsored by
Cleveland Local Section of The Electrochemical Society
The Edison Sensor Technology Center
Resource for Biomedical Sensor Technology
Case Center for Electrochemical Sciences



Proceedings Volume 87-15

IE ELECTROCHEMICAL SOCIETY, INC., 10 South Main St., Pennington, NJ 08534-2896

PROCEEDINGS OF THE SYMPOSIUM ON

SENSOR SCIENCE AND TECHNOLOGY

April 6-8, 1987
Electronics Design Center
Case Western Reserve University
Cleveland, Ohio 44106

Proceedings Editors
B. Schumm, Jr., C. C. Liu, R. A. Powers, and E. B. Yeager

Sponsored by
Cleveland Local Section of The Electrochemical Society
The Edison Sensor Technology Center
Resource for Biomedical Sensor Technology
Case Center for Electrochemical Sciences



Proceedings Volume 87-15

THE ELECTROCHEMICAL SOCIETY, INC., 10 South Main St., Pennington, NJ 08534-2896

symposium and to the Eveready Battery Co., Inc. for permitting significant employee effort to carry out the symposium as well as the Foil Division of Gould, Inc., The Standard Oil Co. and Cortest, Inc.

The sponsors and editors wish to thank the session chairmen, committee members, the speakers and the attendees for their participation in discussions and for providing the papers and edited discussion material. The production of the final printed matter has been dependent on the skilled efforts of Ms. Ruth Ater, Ms. Jean McNulty, Mr. Al Gavlik and Mrs. Doris Tabler who assisted in the preparation of texts and other needs of the symposium.

B. Schumm, Jr.
E.B. Yeager
C.C. Liu
R.A. Powers

CONTENTS

	<u>Page</u>
Preface	111
 SESSION I. Electrochemical Sensors	
Chairman: E.B. Yeager Case Western Reserve University	
Time Responses, Impedances and Transport in Neutral Carrier Sensors	3
R. Buck and M.L. Iglehart University of North Carolina	
Biomedical Applications of Electrochemical Sensors	18
M.R. Neuman Case Western Reserve University	
Integrated Electrochemical Sensors	31
J. Van der Spiegel, I. Lauks, S. Yoder, C. More and J. McKeon, U. of Pennsylvania	
 SESSION II: Fiber Optic Sensors	
Chairman: G. Seng NASA Lewis Labs	
Status of Fiber Optic Sensor Technology	43
J.E. Donovan and C. Gabler Naval Research Laboratories, Washington, D.C.	
New Approaches to Indicators for In Situ Optical Sensing	54
Z. Shaksher, Y. Zhang, D. Sundberg, C.L. Grant and W.R. Seitz University of New Hampshire	
Overview of Flight Sensors Research for Aeronautics	63
R. Baumbick, NASA Lewis Labs	
 SESSION III: Modified Surface and Ion Selective Electrodes	
Chairman: R.A. Powers Edison Sensor Technology Center	
Chemically Modified Electrodes as Biosensors	85
A.M. Yacynych, Sylvia V. Sasso, G.M. Heider and H.J. Wieck Rutgers University	

	<u>Page</u>
Polymer-modified, Carbon Fiber Microelectrodes as Catechol Sensors L.A. Coury, Jr., Eileen M. Birch, and W.R. Heineman	104
Recent Advances in Microelectronic Sensors (Ion Selective Field Effect Transistors) A.K. Covington, Univ. of Newcastle upon Tyne	121
SESSION IV: Micromachining and Microfabrication Techniques	
Chairman: Wen H. Ko Case Western Reserve University	
Thin Film and Chamber Type Sensors O. Prohaska, Case Western Reserve University	131
Advances in Piezoelectric Films and Microstructures R.S. Muller, University of California (Berkeley)	139
Three Dimensional Microstructural Fabrication Technology for Sensor Technology W.H. Ko, Case Western Reserve University	147
Silicon Micromachining: Key to Silicon Integrated Sensors K. Najafi, University of Michigan	152
SESSION X: Novel Sensors	
Chairman: C.C. Liu Case Western Reserve University	
New Technologies for Automotive Sensors I. Igarashi, Toyota Central R&D Labs	167
Surface Acoustic Wave Sensors: Chemiresistor Sensors and Hybrids Using Both Techniques Simultaneously to Detect Vapors W.R. Barger, M.A. Klusty, A.W. Snow, J.W. Grate, D.S. Ballantine, and H. Wohltjen Naval Research Laboratory, Washington, D.C.	198
Continuous Monitoring with Immunosensors W. Schramm, T. Yang, S.H. Palk and A.R. Midgley University of Michigan	218
Index	233
Organization and Sponsors	

SESSION I

ELECTROCHEMICAL SENSORS

TIME RESPONSES, IMPEDANCES AND TRANSPORT IN NEUTRAL CARRIER SENSORS

Michael L. Iglehart and Richard P. Buck

Department of Chemistry

University of North Carolina

Chapel Hill, NC 27514

Following the methods developed for an interfacial process with high resistance electrolyte, an ionic conductor with low resistance electrolytes is modelled. The various effects observed on a PVA membrane are compared with terms in the model. A number of I-t curves are presented. It is found that ohmic behavior is seen at $t=0$ with declining values in a backward "flattened S" shaped function of time, to the steady state. Close agreement with the model is found with a diffusion coefficient determined to be the same by four different methods.

1. INTRODUCTION

Current-time curves of electrochemical systems are generally determined in the course of defining and understanding normal behavior. Current-time curves of metal electrode/electrolyte interfaces show up two of the characteristic phenomena in conventional electrochemistry: mass transport controlled fluxes at reversible interfaces and surface kinetic control of fluxes at electrochemically irreversible interfaces. More complicated kinetic situations can often be diagnosed from deviations of I-t curves from expected behavior of simpler systems. One of these is the case of a reversible interfacial process combined with a high resistance electrolyte treated by Chapman and Newman (1). The results reported in this paper bear a formal resemblance to their system, even though we are dealing with an ionic conductor (the PVC membrane) bathed on two sides by low resistance electrolytes. The neutral carrier PVC membrane behaves as a resistance at short times after application of a voltage step. Subsequently, concentration polarization of the neutral carrier, valinomycin, confers diffusion-control and a limiting current that is generally less, but can approach the short-time ohmic current value.

Mathematically, the two physical systems are coupled in similar ways and give similar I-t curves, although the details of interfacial potentials are quite different.

In the four preceding papers of this series (2-5), the presence of membrane-trapped, anionic, fixed impurity sites in commercial poly(vinyl chloride) (PVC) has been demonstrated by a number of techniques and analysis of resulting electrochemical effects. Ordinarily, the conclusion to be drawn is that the membranes are simply low-site density, fixed-site ion exchangers, and in the absence of Donnan Exclusion Failure conditions, the current-voltage curves would be entirely ohmic at all sensible applied voltages, and current-time curves would be uninteresting constant values for all times after the interfacial double layer charging. As we have shown, the I-V results are quite different and resemble mobile-site ion exchanger curves with limiting currents at applied voltages above the ohmic region (4). These results have been interpreted by the steady-state carrier mechanism in which current at high applied voltages is controlled by consumption and release of neutral carrier at the two membrane-electrolyte interfaces and the consequent linear concentration polarization profile of carrier throughout the membrane.

This paper continues the observations on neutral carrier behavior in low-loaded fixed-site membranes. The basic reversible interfacial potential equations and IR terms are now viewed in the transient state. The flux equation for neutral carrier is developed and the two are analyzed, but not solved to suggest the expected form of the I-t response at applied voltages in the ohmic, transition, and limiting current regions as defined and illustrated in Part IV (5). Unfortunately, this transport problem is nonlinear and defies analytical solution. However, the form of the I-t response at short, and separately at long times can be determined. Dependence of the current on carrier loading and on applied voltage defines the controlling processes and the principal terms in the response

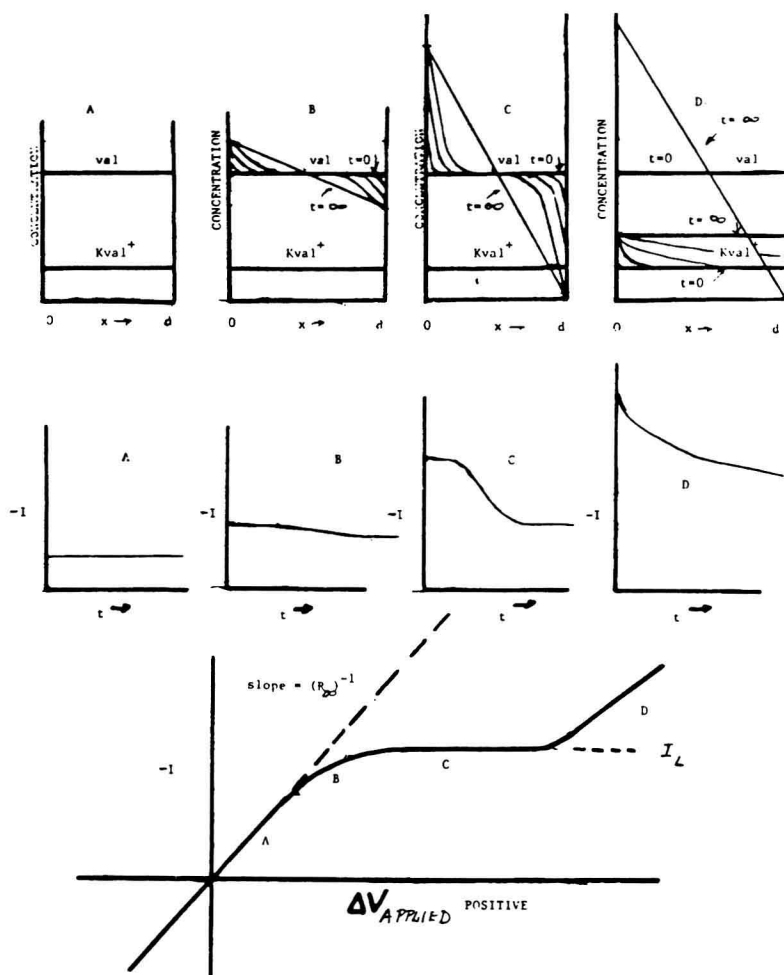


Fig. 1. Composite View of Carrier Concentration Profiles, I-t Curves and Steady State I-V_{Applied} Curve.

Upper Panels A-D, Concentration-Distance Plots

Middle Panels A-D, Current-Time Curves

Lower, Current-Voltage Curve

function.

2. THE MODEL

Normal PVC membranes contain fixed negative sites at low concentrations, 0.05 - 0.5 mM. Typical valinomycin loading is 9mM, and the concentration of $Kval^+$ is the same as the negative sites, while free K^+ is negligibly small. From Part IV(5) the I-V curve is easily divided into 3 or 4 typical parts and there are corresponding I-t curves expected for each I-V segment. The different I-t curves arise from the corresponding free valinomycin concentration profiles and their changes with time. The model is summarized in Fig. 1 where the concentration-distance-time profiles of carrier, corresponding I-t curves, and steady state I-V curves are illustrated.

At low applied voltages A, the I-t curve is a constant (in time) and depends only on applied voltage because current is carried by $Kval^+$ while back diffusion of valinomycin is sufficiently rapid that no appreciable concentration polarization occurs. The length of this region on the applied voltage axis depends on the magnitude of the valinomycin diffusion coefficient.

In regions B and C, the initial current is the appropriate ohmic value determined by applied voltage and resistance of $Kval^+$ motion. At each succeeding period of time, the carrier concentration rises at $x=0$ and decreases at $x=d$ for negative currents (positive applied voltages $V_{Applied} = V_r - V_1$). Note that the constancy of current implies that carrier concentration profiles remain parallel to each other, e.g. have equal slopes at $x=0$ and $x=d$ at each instant of time. At some later time, the surface carrier concentrations reach a steady value and further current flow is connected with the "filling in" of the concentration profile plot to the left of $x=d/2$ and to emptying of the triangle from $x=d/2$ to $x=d$. Eventually, the steady state profile is reached which is linear across the membrane and has a higher value than \bar{V} at $x=0$ and a lower value at $x=d$. The midcell value remains at \bar{V} . \bar{V} is the initial valinomycin concentration, and the spacial average at any time. In B, the surface concentrations or

carriers have not reached the extreme values that correspond to the limiting current. In the limiting current region C, ohmic current at $t=0$ is maintained until the surface concentrations of carrier have risen at $x=0$ to $2\bar{V}$ and reached zero at $x=d$. Current falls while the

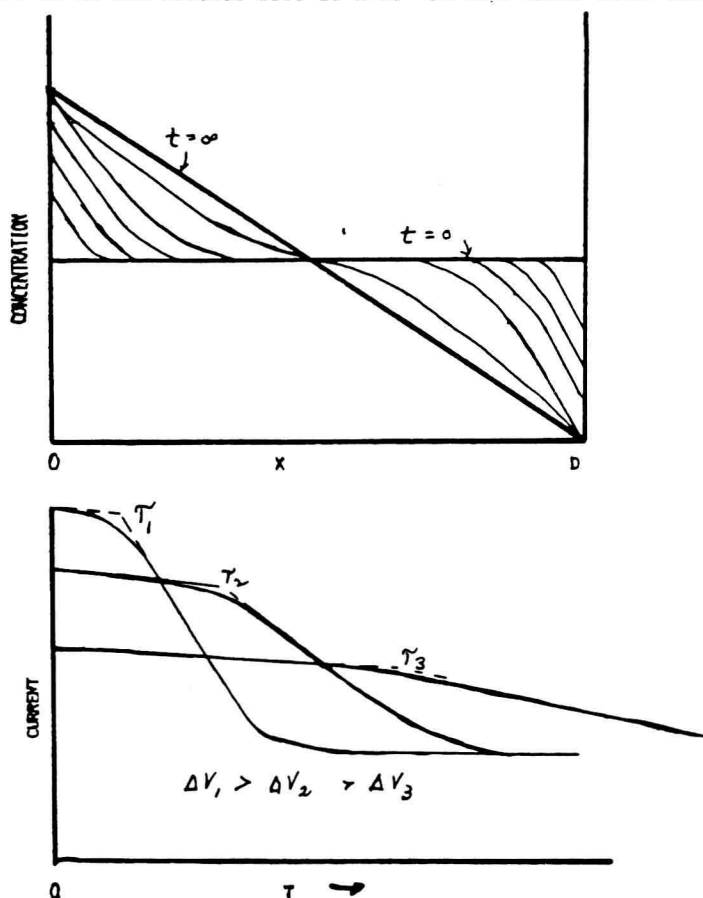


Fig. 2. Schematic Version of Time-Dependent Carrier-Distance Profiles, Carrier Surface Concentrations vs. Time, and Current-Time Plots For Different Applied Voltages Along the Plateau (Limiting) Current.

carrier becomes distributed in a linear way across the membrane. These statements are illustrated schematically in Fig. 2.

These deductions are based on the forms of the equations, and on the experimental results. It is not clear what happens at high applied voltages in region D. The current starts at the ohmic values, but there is an immediate decrease that does not compare with backward running "flattened S" curves for regions A-C. It is likely that anions from the electrolytes are no longer excluded, and the total salt, as $Kval^+ Cl^-$, rises throughout the membrane. This result, in panel D, shows the $Kval^+$ concentration line moving from the low value set by site concentration, to a higher value at each new applied voltage, corresponding to the observed higher steady state currents above the limiting value.

3. THE MODEL MATHEMATICS

In Part III(4), it was shown that the total voltage across the membrane can be expressed as three terms: IR_∞ and two interfacial pds. In the time domain, this equation transformed is

$$V_{Applied}/s = -I(s)R_\infty + \int_0^d (RT/F) \ln[C_v(x=d)/C_v(x=0)] \quad (1)$$

The concentration of valinomycin C_v is subject to two constraints: the total carrier concentration remains constant, and the fluxes at the boundaries are equal and proportional to the current. Thus the boundary concentration transforms have a familiar form

$$C_v(s) = C_v^0/s \pm [I(s)/FA(D_{val}s)^{1/2}] \tanh[(s/D_{val})^{1/2}(d/2)] \quad (2)$$

where the plus applies to $x=d$ and minus to $x=0$. The concentration profile, in the steady state is linear:

$$C_v(x) = C_v(x=0) + [2\bar{V} - 2C_v(x=0)]x/d \quad (3)$$

and the limiting current in the plateau region is

$$I_L = 2FA\bar{V}D_{val}/d \quad (4)$$

This result is found from eq. 2 by passing to the limit of $sI(s)$ as $s \rightarrow 0$. A linear concentration profile of lesser slope can be found at other lower voltages, as well.

Eq. 1 shows that the applied voltage is distributed over two terms. In the ohmic region, eq. 1 is dominated by the IR term

because C_v remains about constant across the membrane for each applied voltage. The transition region occurs when the first term dominates initially, but both terms are comparable in the steady state. In the plateau region, the first term dominates at short times, but the second term controls in the steady state because the concentration, C_v , at one interface approaches zero.

Relatively more complete analysis of the I-t curves can be done for applied voltages in the plateau region C. It happens that the initially ohmic current drives the surface concentrations of carrier to the steady state conditions before the concentration profiles of carrier become perturbed in the membrane interior. One can treat the current-driven build-up at one interface and depletion at the other without worry about interactions because most of the membrane interior maintains a constant carrier concentration. During this initial time period, I remains nearly constant at the ohmic value and the surface concentrations obey approximately

$$C_v(x=0,d) = V \pm 2V_{\text{Applied}} t^{1/2} / \text{FAR}_{\infty} (D_{\text{val}} \bar{n})^{1/2} \quad (5)$$

Defining τ in the usual way,

$$\tau^{1/2} = \text{FA}(D_{\text{val}} \bar{n})^{1/2} / 2(V_{\text{Applied}} / R_{\infty}) \quad (6)$$

the initial period of nearly constant current should persist to time τ according to

$$I = I(t=0) - (RT/\text{FR}_{\infty}) \ln[(1 + (t/\tau)^{1/2}) / (1 - (t/\tau)^{1/2})] \quad (7)$$

These initial current regions, behaving like induction periods, are more abrupt at each increasing applied voltage along the plateau, limiting current region, as shown schematically in Fig. 2. The end of constant current occurs at time τ . Experimentally, the shortening of the induction period is very clear for a series of applied voltages. To prove the effect experimentally, in Fig. 3 is given the apparent τ value (as an inverse square root) against the initial ohmic current value. The τ values are measured by extrapolating $I(t=0)$ to the intersection with the best straight line through the breaking region. Not only do the data

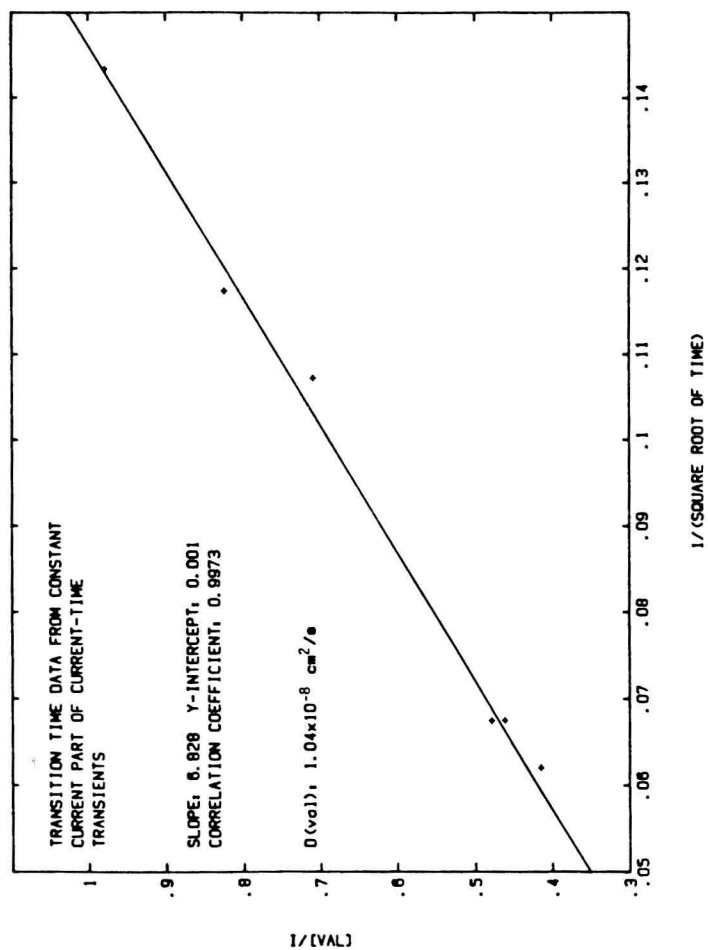


Fig. 3. Plot of $I(t=0)/\bar{V}$ Against Reciprocal Root τ For Several Applied Voltages.

obey the prediction of the constant current hypothesis, but the calculated valinomycin diffusion coefficient agrees with the steady state values.

After the initial constant current region of the I-t plot, current falls abruptly and eventually approaches, asymptotically, the steady state limiting current I_L . This behavior has been treated before (6) and is a standard form in diffusion theory for finite systems. The basic solution follows from inversion of eq. 2 for fixed concentrations at the boundaries. The solution, for long times arises from the exact theta function solution:

$$I(\text{long times}) = I_L (1 + 2\exp(-4\pi^2 D_{\text{val}} t/d^2)) \dots \quad (8)$$

The interesting observation from our experimental data is that the exponential form applies over a very long time period, almost from the transition time, τ .

4. EXPERIMENTAL

The chemicals, apparatus, electrodes and cells, and the procedure were described in Part IV(5).

5. RESULTS

The principal results of this study are the I-t curves for normal membranes at applied voltages in the plateau or limiting current range. An example is shown in Fig. 4. There is an initial current which holds constant for about 250 secs. The current then breaks into a monotonic decrease until the steady state is reached. The initial current is exactly given by the applied voltage divided by the high frequency resistance. Comparison of R_{∞} calculated from $I(t=0)$ with the width of the impedance plane semicircle is given in Table 1. The width of the initial constant current region, reported as τ , is inversely proportional to the square of the initial current, $I(t=0)$. This observation is critical to establishment of the model and is illustrated by the data in Fig. 3. The sharpness of the break-over depends on the precision of surface concentration change

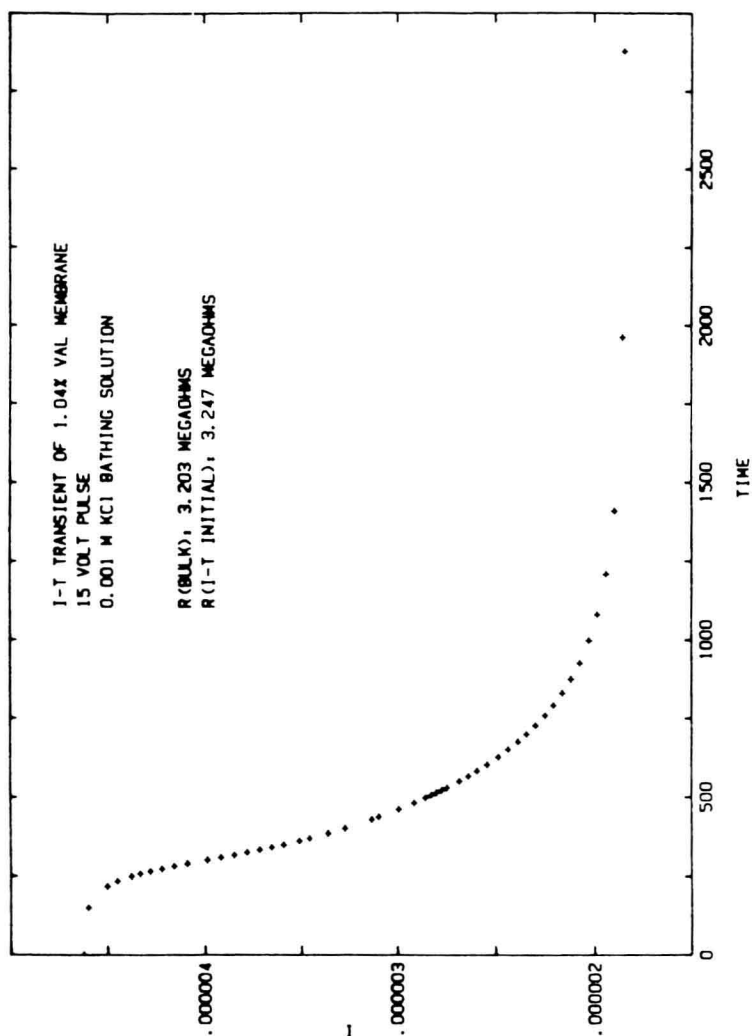


Fig. 4. Current-Time Transient of 1.04% Valinomycin Membrane
 $V_{\text{Applied}} = 15 \text{ V}$; Bathing Electrolytes 0.001 M KCl.